ELSEVIER

Journal of Molecular Catalysis A: Chemical 104 (1996) 319–328

JOURNAL OF MOLECULAR CATALYSIS A: CHEMICAL

Pyridine adsorption onto metal oxides: an ab initio study of model systems

R. Ferwerda [1,a,*], J.H. van der Maas [a], F.B. van Duijneveldt [b]

[a] *Department of Analytical Molecular Spectrometry, Utrecht University, P.O. Box 80.083, 3508 TB Utrecht, Netherlands*

[b] *Department of Theoretical Chemistry, Utrecht University, P.O. Box 80.062, 3508 TB Utrecht, Netherlands*

Received 1 March 1995; accepted 3 June 1995

Abstract

In order to shed some light on the origin of the shifts of the vibrational frequencies of pyridine adsorbed on metal oxides, ab initio calculations have been performed. SCF methods may be used to assign and identify the pyridine vibrations of interest, although coupling of certain vibrational modes hamper the interpretation. The effect of the ligands on the vibrations of pyridine is rather complex. It appeared that the shifts are mainly due to the direct effect of the ligand on the force constants and to changes in the extent of coupling with the in-plane bending vibrations of the hydrogen atoms, and, in case of proton transfer, the N–H group. Protonation, however, severely influences the geometry of pyridine, which may also have a considerable effect on the vibrational frequencies.

1. Introduction

Pyridine is often used as a probe molecule to examine the acidity of metal oxide catalysts. Owing to its electron donor capabilities, the strength of electron pair acceptor sites can be monitored [1–5]. These sites can be studied with infrared spectroscopy in the region 1700 to 1400 cm^{-1}. In this part of the spectrum, where most metal oxides show an infrared window, pyridine has strong absorptions, i.e. ν_{8a}, ν_{8b}, ν_{19a} and ν_{19b} following Wilson's mode number for the assignment of the vibrations of benzene [6].[2] These modes are weak in Raman spectroscopy, where the ring breathing region (ν_1 and ν_{12} modes) is a better choice to study the interactions of pyridine with surfaces.

Adsorption of pyridine at different acidic sites may result in a change in centre, intensity and profile of the vibrational bands as compared to the corresponding bands in the free, unperturbed molecule. The general position of a specific vibration of pyridine interacting with a given type of adsorption site can be found from model systems. When pyridine interacts with an acid site, the frequency of the ring vibrations is seen to increase, which corresponds to a strengthening of the bonds leading to increased force constants. The assignment of the vibrational modes of pyridine adsorbed on different sites is presented in Table 1.

We operationally define a Brønsted site as an OH group which is, at room temperature, acidic enough to transfer its proton to pyridine forming

* Corresponding author.

[1] Present address: ATI Unicam, York Street, Cambridge, CB1 2PX, UK.

[2] Although these benzene modes are degenerate, the corresponding pyridine vibrations may show slightly different energy.

SSDI 1381-1169(95)00179-4

Table 1
Vibrational frequencies of the infrared (ν_{8a}, ν_{8b}, ν_{19a}, ν_{19b}) [1] and Raman (ν_1, ν_{12}) [16,18] modes (cm^{-1}) of pyridine used in the characterisation of surfaces as determined from model systems. Argon matrix values from [30]. Assignment of modes according to Wilson [6].

Mode	Symm.	Ar matrix	Liquid	Hydrogen bonded	Brønsted sites	Lewis sites
ν_{8a}	A_1	1582	1582	1590–1600	1640	1600–1633
ν_{8b}	B_2	1577	1575	1580–1590	1620	1580
ν_{19a}	A_1	1483	1482	1485–1490	1485–1500	1488–1503
ν_{19b}	B_2	1441	1438	1440–1447	1540	1447–1460
ν_{12}	A_1	1031	1031	1032–1040	1025–1035	1040–1050
ν_1	A_1	991	991	996–1005	1007–1015	1016–1028

a pyridinium ion, whereas association with an OH site will be referred to as hydrogen bonded pyridine. In the literature [2,4,7,8] the interaction between pyridine and OH groups (hydrogen bonded pyridine) is often described as 'physisorbed'. Following adsorption at lower temperatures ($<100°C$), however, pyridine species are observed which have (almost) liquid-like features and we would like to adopt the word 'physisorbed' for these, i.e. indicative of a weak (non-specific) association. The different interactions are depicted in Fig. 1.

The assignments provided in Table 1 are usually used as a guide for the interpretation of the vibrational spectra of pyridine adsorbed onto metal oxides. The literature, however, indicates that discrepancies exist between different authors, and the Raman spectra are most often not compared with infrared results [9–22]. The situation is further complicated by the fact that the shifts and relative intensities of the ring modes of adsorbed pyridine in infrared and Raman spectroscopy seem to depend on the nature of the catalyst, thus making the assignment of bands even more difficult [23–26].

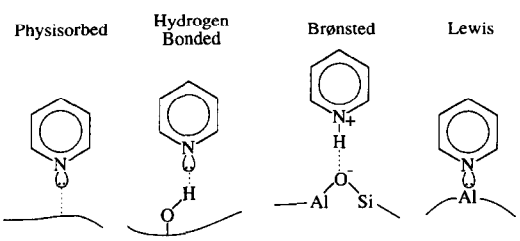

Fig. 1. The different interactions of pyridine with zeolite surfaces.

Theoretically, the origin of the shifts of pyridine has not been fully elucidated. A model in which the donation of electrons from the nitrogen lone pair to the ligand orbitals decreases the π or σ electron density in the ring would predict negative shifts upon complexation, whereas a blue shift is observed. Ab initio methods may be used to study the association of pyridine with probe molecules and to analyse the effect of complexation on the vibrations of the aromatic. In 1975, Del Bene [27] performed SCF calculations using the STO3G basis set on hydrogen bonded pyridine complexes. An SCF/4-31G study of the vibrational changes upon protonation of pyridine was published by Ajito et al. [28]. Wiberg [29] calculated the vibrational spectrum of pyridine using the 6-31G* and 6-31+G* basis sets. Recently, Destexhe et al. [30] reported on the experimental vibrational shifts of matrix isolated pyridine and pyridine–water, together with its SCF/6-31+/+G** predicted frequencies.

In the present work, we report on quantum chemical calculations of the vibrational frequencies of pyridine and several pyridine complexes. The main goal of this work was to identify and assign the different vibrational modes used in the studies of pyridine adsorbed onto surfaces. Furthermore, the effect of the ligand on the nature and frequency of the vibrations has been examined and additionally, the use of SCF calculations has been assessed. Finally, we have tried to rationalise the changes and shifts which occur upon complexation.

It is emphasised that the calculations are by no means intended to mimic the 'real' situation, i.e. to give complete agreement with experiment. The main purpose of the present quantum chemical calculations is to provide some understanding of the shifts observed in the Raman and infrared spectra of pyridine adsorbed onto metal oxides.

2. Method of ab initio calculations

The complexes of pyridine with H_2O, the dimer of water, NaCl and HCl, and its protonation were selected as model systems for our calculations. The computations were carried out at the restricted Hartree–Fock level with the ab initio program GAMESS-UK [31,32] on an HP 7500 system. Computation of the vibrational frequencies was performed by calculating the analytical second derivatives of the energy surface. In general, geometries were optimised with the STO3G basis set, and the vibrational frequencies were calculated then with the 6-31G* basis set. The latter basis set was preferred for the calculations of the frequencies, because the work of Wiberg [29] showed that the band positions of pyridine are in reasonable agreement with the experimental values, after correction for anharmonicity and overestimation of the force constants by the SCF procedure (by using a scaling factor of approximately 0.9). No attempts were made to correct for the basis set superposition error (BSSE). It has been shown that at a given geometry of the complex, the BSSE has only a small effect on the stretching frequencies in SCF calculations [33]. This leaves, however, the possibility that the STO3G estimated geometry of the complexes is affected by the BSSE [34] and this will be addressed to below.

The geometries were constrained to the highest possible symmetry. Hence, except for the pyridine–water compounds, all complexes possessed C_{2v} symmetry. The C_s symmetry was adopted for the pyridine–H_2O complex, i.e. with the plane of the water molecule perpendicular to the plane of the ring, which is energetically the most favourable conformation [27,34]. We assumed that the pyridine–water dimer complex would maintain this symmetry, with the second water molecule in the same plane as the first one (and thus perpendicular to the plane of the pyridine ring).

3. Results and discussion

3.1. The ring vibrations of pyridine

The STO3G optimised geometry of pyridine is displayed in Fig. 2a. A comparison with the cor-

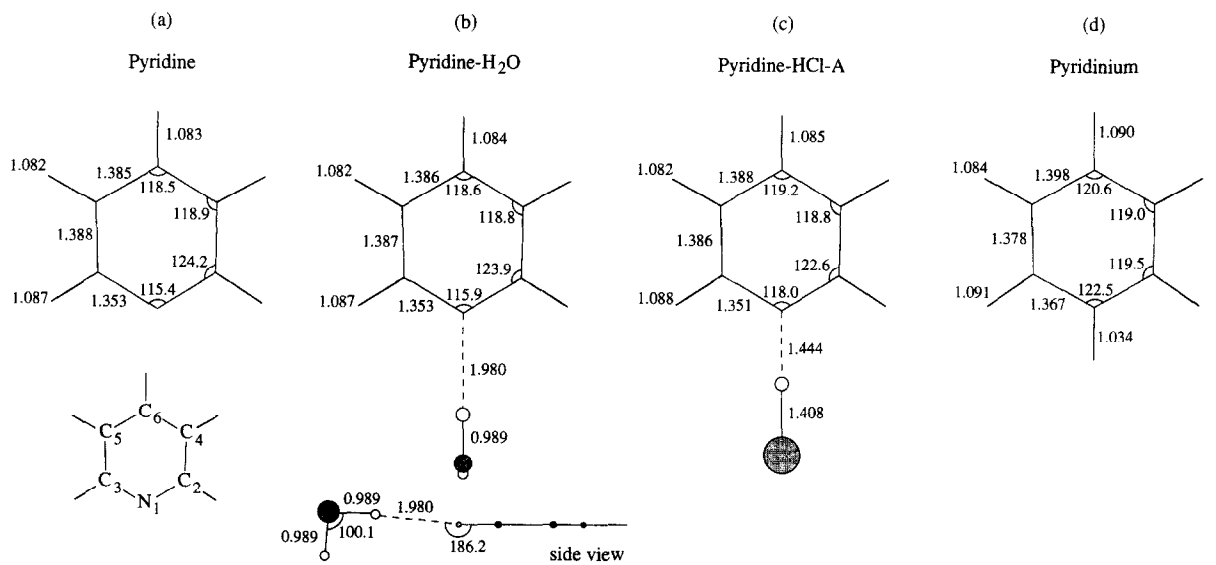

Fig. 2. Calculated geometries of pyridine and its complexes (for details see text). Bond lengths are in Å, bond angles in °.

Table 2
Experimental geometries of pyridine and pyridinium chloride

Pyridine [40]				Pyridinium chloride [28]			
Bond length	(Å)	Angle	(°)	Bond length	(Å)	Angle	(°)
N_1–CO_2	1.338	C_3–N_1–C_2	116.9	N_1–C_2	1.32	C_3–N_1–C_2	128
C_2–C_4	1.394	N_1–C_2–C_4	123.8	C_2–C_4	1.42	N_1–C_2–C_4	118
C_4–C_6	1.392	C_2–C_4–C_6	118.5	C_4–C_6	1.40	C_2–C_4–C_6	115
C_2–H	1.086	C_4–C_6–C_5	118.4	C_2–H	–	C_4–C_6–C_5	125
C_4–H	1.086			C_4–H	–		
C_6–H	1.081			C_6–H	–		

responding experimental values (Table 2) reveals that the obtained geometry is in reasonable agreement with experiment, which was also observed by Del Bene [27].

Table 3 presents the 6-31G* calculated wavenumbers of the normal vibrations used in vibrational spectroscopy studies of pyridine adsorbed onto metal oxides. The assignments are based on a visual inspection of the displacements vectors of the atoms for the vibrations of interest (Fig. 3).

Examination of the calculated wavenumbers for pyridine shows that the frequencies are overestimated by approximately 10%, which corresponds with earlier work [28,29]. Scaling factors were determined, following Ajito et al. [28], by dividing the experimental value by the calculated one. These factors were used to correct the computed wavenumbers of the pyridine complexes and the pyridinium ion, which has been rationalised on the concept of the group frequency [28].

Compared to the normal vibrations of benzene, it appears that the modes of the pyridine ring have acquired some character of the in-plane hydrogen bending modes, i.e. some coupling (mixing) takes place. According to the present calculations, the vibrations used in Raman (ν_1 and ν_{12}) are mixed with ν_{18a}, viz. a symmetric in-plane bending vibration of the hydrogens (observed at 1073 cm^{-1} in the unperturbed molecule [30]). A similar behaviour is observed for the infrared active modes, which show a large contribution of in-plane bending vibrations of the hydrogens. Note that this effect may affect the shifts upon complexation. When the frequencies of the vibrations of pyridine alter due to association with another molecule, it is possible that the extent of the coupling changes, resulting in turn in a shift of the frequency. Therefore, the observed differences may be brought about by a mutation in the nature of the normal mode, rather than reflecting the effect of, for example, water upon the force constants or the geometry of pyridine.

As shown in Fig. 3, the ν_1 mode is mainly dependant on the force constants of the ring system, whereas the ν_8 and ν_{19} modes are also severely influenced by the hydrogen vibrations.

3.2. Complexation of pyridine with water

In order to assess the usefulness of SCF calculations in the determination of the vibrational shifts of pyridine complexes, the frequencies of several pyridine–H_2O complexes were calculated

Table 3
Calculated and scaled frequencies (cm^{-1}) of pyridine upon interaction with water. Experimental values from Table 1. For an explanation of the complexes, see Fig. 2 and text

Mode	Pyridine			··H_2O	··H_2O	··Dimer	H_2O··H_2O	Pyr–H_2O
	Exp.	Calc.	Scaling		2.2 Å			experimental
ν_1	991	1058	0.937	999	995	1002	1000	996–1005
ν_{12}	1031	1121	0.919	1034	1032	1035	1036	1032–1040
ν_{19b}	1441	1585	0.909	1443	1444	1445	1454	1440–1447
ν_{19a}	1483	1648	0.900	1486	1485	1487	1486	1485–1490
ν_{8b}	1577	1752	0.900	1578	1578	1579	1587	1580–1590
ν_{8a}	1582	1782	0.888	1585	1584	1586	1584	1590–1600
ν_{18a}	1073	1167	0.919	1074	1074	1074	1073	–

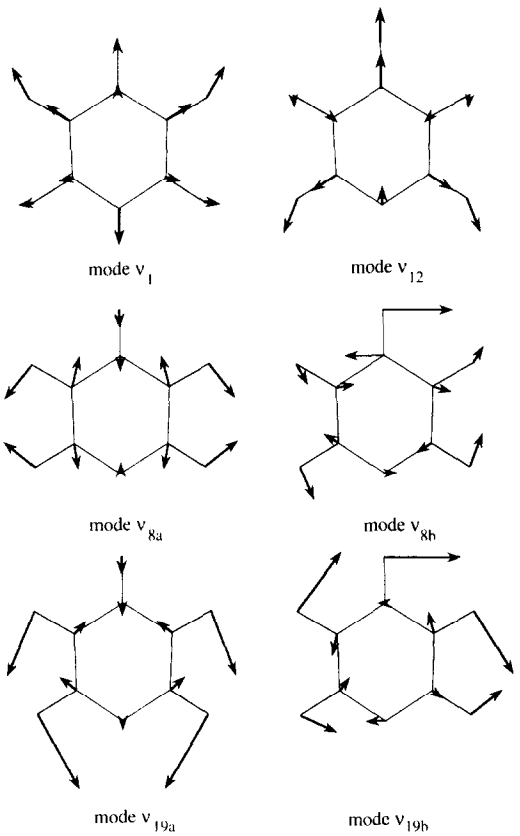

Fig. 3. Vibrations of pyridine of interest for studies of pyridine adsorbed onto acidic surfaces, as calculated with SCF/6-31G* // STO3G (The last basis set defines the one used for optimisation of the geometry, whereas the first one was used for computation of the frequency). The displacement vectors are multiplied by 10.

and compared with those of unperturbed pyridine. The calculations were performed in a number of separate steps to partition the effects which lead to certain shifts [33]. It appears that association with water hardly influences the character of the modes under consideration. The frequency of the ν_1 mode is considerably affected, whereas all other vibrations reveal similar, though more moderate effects (Table 3). Therefore, we will mainly focus on the ν_1 mode.

Fig. 2b shows the STO3G calculated conformation of the pyridine–water complex. Remember that the use of this minimal basis set may lead to errors in the geometry as it gives too short intermolecular separations for hydrogen bonded complexes [34]. As expected, re-optimisation of the geometry of this complex with the 6-31G* basis set computes a N···H distance of 2.121 Å, some 0.14 Å longer than at the STO3G level.

The blue shift of several wavenumbers upon complexation of pyridine with water coincides with experimental observations (Table 3). When using SCF/6-31+/+G** for optimisation of the geometry and frequency calculation of the pyridine–H_2O complex, the same trend was observed [30]. In that study the ν_1 mode shifts +4 cm^{-1} upon complexation as compared to the shift of +8 cm^{-1} in the present 6-31G*//STO3G work. When the 6-31G* basis set is applied for optimisation of the geometry of both pyridine and pyridine–H_2O, prior to the calculation of the frequency, a shift of +5 cm^{-1} is found. We attribute these differences to the elongation of the N···H distance upon using a larger basis set. The frequency of the STO3G optimised pyridine–H_2O complex with the hydrogen of water positioned at a distance of 2.2 Å from the nitrogen of pyridine was calculated in order to check the influence of the N···H distance on the frequency shift. Again, the same trend is observed, and the perturbations of the vibrations of the molecule are now smaller (the ν_1 mode shifts +4 cm^{-1} only, Table 3). This indicates that the calculated shifts are sensitive to the length of the hydrogen bond.

The shift of a few more wavenumbers of the ν_1 mode in the pyridine–water dimer complex (Table 3) agrees well with the observed values in these kind of systems [35–37]. This is often attributed to the induction effect of the second water molecule on the acidity of the associating proton, but it may also be due to the decrease of the N···H distance by 0.13 Å.

The frequency shifts are provoked by the change in the geometry of pyridine ($\Delta k_{\text{indirect}}$) and by the direct effect of the ligand on the force constants of the ring originating from the non-zero second derivatives of the interaction energy of the dimer – retaining the unperturbed pyridine geometry (Δk_{direct}) [33]. In order to determine the relative importance of these mechanisms, ab initio calculations of pyridine with the geometry of pyridine–H_2O, and of the pyridine–H_2O complex with the geometry of pyridine were performed.

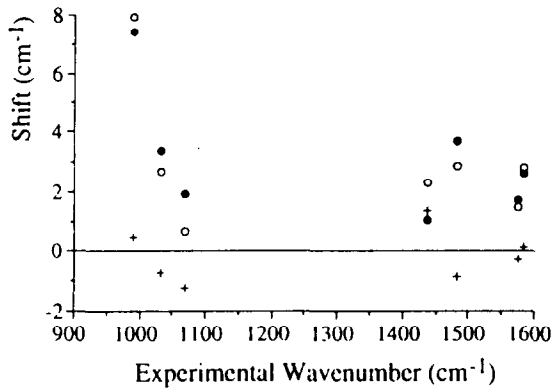

Fig. 4. Effect of association with water, with and without change of geometry according to optimisation with STO3G and frequency calculation at the 6-31G* level. (○) Pyridine–water, geometry of complex optimised with STO3G, (●) Pyridine–water, with the geometry of pyridine, and (+) Pyridine, with the geometry of the pyridine–water complex.

Fig. 4 shows the shifts upon complexation as compared to the unperturbed molecule, after scaling by the factor of approx. 0.9. Obviously, the effect of the geometry change ($\sim 1\ cm^{-1}$) is smaller than the direct effect of water on the force constants (Δk_{direct}) of the complex.

Ajito et al. [28] found that the optimised structure of pyridine in the water complex obtained by SCF/4-31G calculations scarcely deviated from pyridine itself. They suggested that hydrogen bond formation with more molecules need to be considered in order to obtain the vibrational frequencies. It now becomes evident that not the change in geometry is the determining factor, but the direct effect of water on the force constants of pyridine.

Interaction of one water molecule with the lone pair and another one with the hydrogen at the para carbon atom of pyridine reveals the same trends, i.e. a slight deviation of the geometry and small blue shifts of the frequencies ($H_2O\cdot\cdot H_2O$, Table 3). The B_2 normal modes (the ones antisymmetric with respect to C_2 and σ_v) show larger shifts as the hydrogen atom at the para carbon atom plays an important role in these normal vibrations (see Fig. 3).

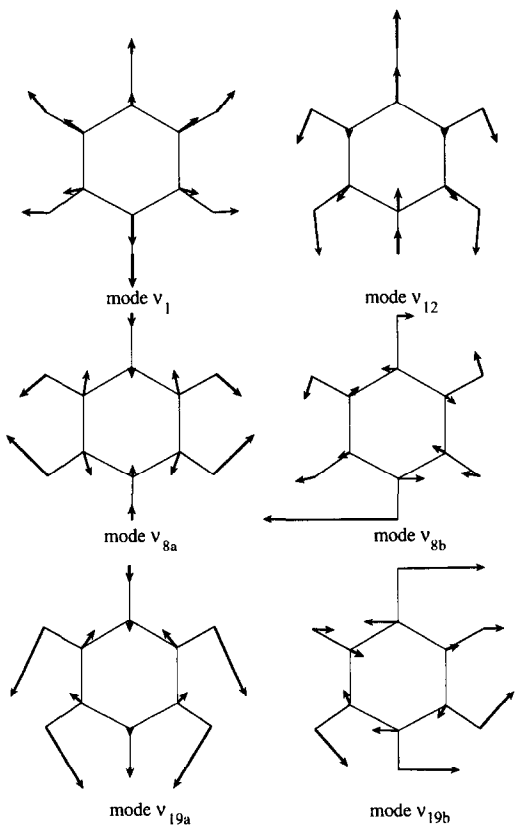

Fig. 5. Normal vibrations of pyridinium ($\cdot\cdot H^+$–A), which are of interest for studies of pyridine adsorbed onto acidic surfaces, as calculated with SCF/6-31G*//STO3G. The displacement vectors are multiplied by 10.

3.3. The effect of protonation on the vibrations of pyridine

The STO3G optimised geometry of pyridine is severely affected by protonation (Fig. 2d). Furthermore, the character of the B_2 modes, viz. ν_{8b} ($1575\ cm^{-1}$) and ν_{19b} ($1438\ cm^{-1}$), is seriously influenced by the transfer of the proton to the nitrogen (Fig. 5). It seems that the in-plane bending vibration of the N–H group affects the character of these normal modes (vide infra), which is also reflected in the large change in frequency of these modes (see $\cdot\cdot H^+$–A, Table 4). The character of the other normal vibrations hardly varies, and their shifts are mainly induced by changes in the force constants and/or the geometry of the ring.

In order to evaluate the different effects (Δk_{direct} and $\Delta k_{indirect}$) on protonation, we calculated the vibrations of pyridinium with the geometry of pyridine ($\cdot\cdot H^+$–B), and of pyridine with

Table 4
Calculated and scaled frequencies (cm^{-1}) of protonated pyridine and after interaction with HCl and NaCl. Experimental values from Table 1. For an explanation of the complexes, see Fig. 2 and text

Mode	Pyridine		··H^+	··H^+	··HCl	··HCl	··HCl	··NaCl	Brønsted
	Exp.	$GeoPH^+$	A	B	A	B	C		exp.
ν_1	991	968	976	991	1033	988	1005	1022	1007–1015
ν_{12}	1031	1012	1029	1041	1045	1022	1025	1046	1025–1035
ν_{19b}	1441	1455	1559	1558	1453	1548	1549	1446	1540
ν_{19a}	1483	1453	1478	1498	1490	1473	1484	1492	1485–1500
ν_{8b}	1577	1542	1609	1615	1579	1571	1591	1574	1620
ν_{8a}	1582	1580	1583	1585	1590	1595	1597	1593	1640
ν_{18a}	1073	1032	1047	1084	1076	1040	1060	1074	

the geometry of pyridinium (pyridine $GeoPH^+$, Table 4).

In the ··H^+–B case, again large shifts of the B_2 modes are observed as compared to neat pyridine. Furthermore, all frequencies shift to higher energy, except that of the ν_1 mode. This latter effect is probably caused by the apparent weight change of the N–H entity, since the replacement of ^{14}N by its isotope ^{15}N shifts the ν_1 mode considerably further down than the other vibrations (12 cm^{-1} versus less than 5 cm^{-1}).

Changing the geometry of pyridine to the one of the pyridinium ion results in frequencies of lower energy. The ν_{18a} mode in particular shows a considerable red shift, which may affect the coupling with the ν_1 and ν_{12} modes. Examining the character of the ν_{12} mode of pyridinium (Fig. 5) and pyridine (Fig. 3), clearly shows the additional contribution of the in-plane hydrogen bending vibrations, indicating that this change in coupling might well take place. These wavenumbers should therefore be used with care. Obviously, the change in geometry of the pyridinium cation ($\Delta k_{indirect}$) is of great importance for the computed wavenumbers.

In practice, the charge of the pyridinium entity is balanced by an anion in its vicinity (for zeolite surfaces, the Si–O^-–Al unit). Therefore, we decided to add a chloride ion to compensate for the positive charge. Upon optimisation of the geometry of this complex with the STO3G basis set (··HCl–A, Table 4), the distance between the nitrogen and proton is 'overestimated', and proton transfer does not occur (Fig. 2c). However, this kind of calculations is based on gas phase complexes and in practice the solvation effect of the matrix (i.e. the molecules/surface in the vicinity of the complex) may induce proton transfer. To mimic this situation, we performed calculations on two more pyridinium–Cl complexes. Firstly, a chloride ion was added to the (STO3G optimised) pyridinium at the same N··Cl distance as in the pyridine··HCl–A complex, prior to 6-31G* calculation of the vibrational frequencies (··HCl–B, Table 4). Secondly, the geometry of the pyridine molecule of the latter complex was optimised at the STO3G level, while the N··H and H··Cl distances were fixed (··HCl–C, Table 4). Table 4 displays the computed values after scaling with the 0.9 factor. The influence of the transfer of the proton to the ring on the nature of the ν_{19b} mode is shown in Fig. 6.

Addition of a charge-balancing anion to pyridinium (compare ··H^+–A and ··HCl–B) causes the vibrations to shift to lower frequencies. There are, however, two exceptions, viz. the ν_1 and ν_{8a} mode which shift to higher frequencies. Relaxation of this complex (compare ··HCl–B and ··HCl–C) results in upward shifts of all vibrations. A similar behaviour was observed upon relaxation of the pyridinium cation, once more indicating that the geometry change of pyridine to pyridinium substantially affects the frequencies of the vibrations.

Fig. 6 shows that upon transfer of the proton to the ring, the character of the ν_{19b} mode changes

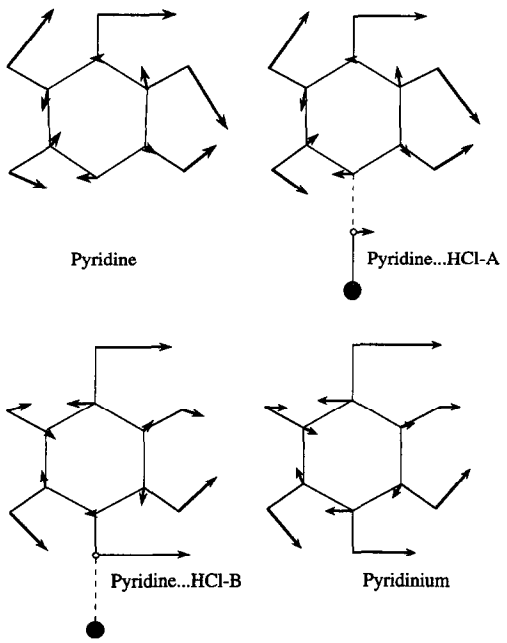

Fig. 6. Change of ν_{19b} mode upon association with HCl. The displacement vectors are multiplied by 10. For an explanation of the different complexes, see text.

considerably. The N–H bending vibration becomes more prominent and simultaneously the direction of the motion of four carbon atoms (C_2, C_3, C_5 and C_6) and of two hydrogens (at carbon atom C_3 and C_5) changes. The ν_{8b} mode shows a similar behaviour, although the effect is smaller. It appears that the ν_{19b} mode strongly couples with the in-plane bending of the N–H group – which is computed at about 1300 cm^{-1} after scaling. However, the coupling between the vibrations is further complicated since the antisymmetric in-plane bending mode of the hydrogens (ν_{14} mode observed at 1363 cm^{-1} [30] and calculated – after scaling with a factor of 0.9 – at about 1370 cm^{-1}), also affects the B_2 modes.

The nature of ν_{19a} and ν_{8a} modes hardly varies, which is confirmed by the relatively smaller frequency shifts. Considering the complexes with 'pyridinium' geometry (pyridine GeoPH$^+$, $\cdot\cdot$H$^+$–A and $\cdot\cdot$HCl–B) and their 'pyridine' geometry counterparts (pyridine, $\cdot\cdot$H$^+$–B and $\cdot\cdot$HCl–C, respectively), we conclude that the shift of the ν_{18a} mode to lower frequency (and thus the change in coupling with the ν_1 and ν_{12} mode) is mainly due to the large change of the geometry of the pyridinium cation as compared to that of pyridine, i.e. $\Delta k_{\text{indirect}}$.

It seems that relaxation of the pyridine ring and proton transfer in the pyridinium chloride complex ($\cdot\cdot$HCl–C, Table 4) is crucial to achieve an adequate description of the effect of a Brønsted site on the vibrations of pyridine. A comparison of the calculated (and scaled) wavenumbers of the pyridine$\cdot\cdot$HCl–C complex with the experimental values reveals that the shifts of the ν_1, ν_{12} and ν_{19} modes are reasonably well reproduced. The ν_{8a} and ν_{8b} modes, however, show large discrepancies compared to the experimental values. Wong and Colson [38] mentioned that these modes are Fermi-perturbed, which might explain the observed disparity, as this is not included in the harmonic vibrational analysis. Furthermore, the literature values are determined from surface complexes and it is possible that these modes are mixed with the vibrations of surface species, e.g. the bending mode of adsorbed water.

Fig. 7 shows the geometry of pyridine$\cdot\cdot$HCl–C. It appears that especially the length of the C–N bond (a shortening from 1.367 to 1.353 Å) changes upon optimisation of the geometry, while the bond angles of the pyridine ring hardly differ from those of the pyridinium ion.

The proton of HCl is not transferred to the pyridine ring upon association and optimisation of

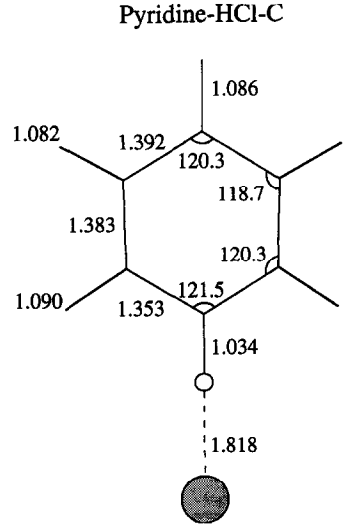

Fig. 7. STO3G optimised geometry of the pyridine$\cdot\cdot$HCl–C complex, with the proton and chloride ion placed at fixed positions.

the geometry of the total complex with the STO3G basis set (··HCl–A). Although the frequencies of the normal vibrations are severely affected, their character is hardly changed. As outlined for the pyridine··H_2O complex, the observed shifts are mainly caused by the direct effect of the associating molecule, which is approx. 5 times larger in the HCl complex than in the one with H_2O. The same trends are observed in a complex like pyridine–NaCl (weak Lewis site, N··Na = 2.075 Å; Na··Cl = 2.287 Å) and the observed shifts are attributed to the direct effect of the ligand on the force constants of the ring (Table 4).

3.4. *Effect of complexation on the vibrations of pyridine*

Several theories have been postulated to explain the shifts observed upon complexation of pyridine. According to Crookell [5], the high pK_b of pyridine suggests that the lone pair lies at some small angle out of the plane of the ring. Therefore, it is possible that the lone pair donates electrons to the lowest unoccupied molecular π orbital, which is anti-bonding, resulting in a lowering of the force constants of the bonds in the ring. Association with specific sites which use the electrons of the lone pair, would remove the possibility to donate electrons into the anti-bonding orbital, thus raising the vibrational frequencies. In our work, however, no interaction with the π system is possible since the free pyridine molecule was taken to be planar, and since the frequency shifts are reasonably well predicted, another explanation is needed therefore.

Emsley (protonation) [39] and Del Bene (interactions with HF and H_2O) [27] showed that complexation results in substantial variations of the σ electron density and a polarisation of the π cloud towards the nitrogen atom of the pyridine ring. According to them, the electron redistribution leads to an increased ionic attraction between nitrogen and adjacent carbon atoms resulting in an increased bond strength and a decreased C–N bond length. In this work, the same polarisation effect is observed, though it is most pronounced in the π cloud of the pyridinium ion, where the frequency of the breathing vibrations is lowered and the distance between the nitrogen and carbon atoms is increased (··H^+–A, Table 4 and Fig. 2). This suggests that the polarisation of the π system of the ring is not (only) responsible for the observed frequency shifts. A further partitioning of the effects which lead to the frequency shifts, i.e. first-order and second-order interaction energies and their individual contributions could give more insight into the relative importance of these kind of changes.

In our opinion the shifts have to be attributed to a combination of effects. When we focus on the ν_1 mode (A_1 symmetry, Table 3 and Table 4), some principal features are apparent; (i) association with either H_2O, NaCl or HCl as well as (ii) optimisation of the pyridine geometry in the pyridinium–Cl complex results in blue shift, whereas (iii) protonation induces a red shift. Thus, association with a small neutral molecule or with a proton leads to an upward shift of the ring breathing mode, i.e. an increase in force constants. As we have shown, this is due to the direct effect of the ligand rather than to the (small) change of geometry. A red shift is calculated when the geometry of the molecule changes from the 'pyridine' to the 'pyridinium' geometry. In case of the ν_1 and ν_{12} modes, this seems to be mainly due to the shift of the ν_{18a} mode to lower wavenumber, resulting in a change of coupling between these modes.

Similar effects are observed for the modes used in infrared assays, although the B_2 modes are severely affected by the transfer of the proton to the ring too. This results in a prominent contribution of the N–H group to the antisymmetric normal vibrations and a simultaneous change of the nature of the ring vibration which accounts for the observed shifts.

4. Conclusions

The calculations presented in this work demonstrate that it is possible to use ab initio methods

to identify the vibrations of pyridine used in the characterisation of surfaces. However, the assignments might be hampered by the coupling of vibrations with the same symmetry. Note that this effect may lead to frequency shifts upon complexation which are caused by deviations in coupling, and therefore the outcome of the calculations should be handled with care.

SCF methods may be applied to predict the variation in character and frequency of the normal vibrations of pyridine upon complexation as long as the experimental vibrations are not disturbed by Fermi resonance. A minimal basis set for optimisation of the geometry of pyridine and its complexes may be used to calculate the frequency shifts with the 6-31G* basis set.

The effect of different ligands on the normal vibrations of pyridine is rather complex. The calculations presented here demonstrate that the shifts depend on three principal features: (i) the direct effect on the force constants of the ligand (which depends on the length of the hydrogen bond), (ii) the change in the geometry of pyridine (mainly the C–N bond length), and (iii) the coupling with the in-plane bending vibration of the hydrogens of the pyridine ring and – in case of proton transfer – the N–H group.

References

[1] E.P. Parry, J. Catal., 2 (1963) 371.
[2] M.R. Basila, T.R. Kantner and K.H. Rhee, J. Phys. Chem., 68 (1964) 3197.
[3] J.A. Lercher, G. Ritter and H. Vinek, J. Colloid Interface Sci., 106 (1985) 215.
[4] L.M. Parker, D.M. Bibby and G.R. Burns, J. Chem. Soc., Faraday Trans., 87 (1991) 3319.
[5] A. Crookell, Ph.D. Thesis, University of Southampton, 1989.
[6] E.B. Wilson, Phys. Rev., 45 (1934) 706.
[7] C.U.I. Odenbrand, J.G.M. Brandin and G. Busca, J. Catal., 134 (1992) 505.
[8] M. Niwa, N. Katada and Y. Murakami, J. Catal., 134 (1992) 340.
[9] J.M. Stencel, Raman Spectroscopy for Catalysis, Van Nostrand Reinhold, New York, 1990.
[10] P.J. Hendra, J.R. Horder and E.J. Loader, J. Chem. Soc., Chem. Commun., (1970) 563.
[11] R.O. Kagel, J. Phys. Chem., 74 (1970) 4518.
[12] P.J. Hendra, J.R. Horder and E.J. Loader, J. Chem. Soc. (A), (1971) 1766.
[13] T.A. Egerton, A.H. Hardin, Y. Kozirovski and N. Sheppard, J. Chem. Soc., Chem. Commun., (1971) 887.
[14] P.J. Hendra and E.J. Loader, Trans. Faraday Soc., 67 (1971) 828.
[15] T.A. Egerton, A.H. Hardin, Y. Kozirovski and N. Sheppard, J. Catal., 32 (1974) 343.
[16] P.J. Hendra, I.D.M. Turner, E.J. Loader and M. Stacey, J. Phys. Chem., 78 (1974) 300.
[17] T.A. Egerton and A.H. Hardin, Catal. Rev., Sci. Eng., 11 (1975) 71.
[18] R.P. Cooney, G. Curthoys and N. The Tam, Adv. Cat., 24 (1975) 293.
[19] T.A. Egerton, A.H. Hardin and N. Sheppard, Can. J. Chem., 54 (1976) 586.
[20] C.P. Cheng and G.L. Schrader, Spectrosc. Lett., 12, (1979) 857.
[21] G.L. Schrader and C.P. Cheng, J. Phys. Chem., 87 (1983) 3675.
[22] M.B. Sayed and R.P. Cooney, J. Colloid Interface Sci., 96, (1983) 381.
[23] M.H. Healy, L.F. Wieserman, E.M. Arnett and K. Wefers, Langmuir, 5 (1989) 114.
[24] W. Hertl, Langmuir, 5 (1989) 96.
[25] C. Morterra and G. Cerrato, Langmuir, 6 (1990) 1810.
[26] A.V. Kiselev and V.I. Lygin, Infrared Spectra of Surface Compounds, John Wiley & Sons, New York, 1975.
[27] J.E. Del Bene, J. Am. Chem. Soc., 97 (1975) 5330.
[28] K. Ajito, M. Takahashi and M. Ito, Chem. Phys. Lett., 158 (1989) 193.
[29] K.B. Wiberg, J. Mol. Struct., 244 (1990) 61.
[30] A. Destexhe, J. Smets, L. Adamowicz and G. Maes, J. Phys. Chem., 98, (1994) 1506.
[31] GAMMESS-UK is a package of ab initio programs written by M.F. Guest, J.H. van Lenthe, J. Kendrick, K. Schoffel, P. Sherwood and R.J. Harrison, with contributions from R.D. Amos, R.J. Buenker, M. Dupuis, N.C. Handy, I.H. Hillier, P.J. Knowles, V. Bonacic-Koutecky, W. von Niessen, V.R. Saunders and A.J. Stone. The package is derived from the original GAMMESS code.
[32] M. Dupuis, D. Spangler and J. Wendoloski, NRCC Software Catalog, Vol. 1, Program No. QG01 (GAMESS), 1980.
[33] J.G.C.M. van Duijneveldt-van de Rijdt and F.B. van Duijneveldt, J. Comp. Chem., 13 (1992) 399.
[34] G. Alagona, C. Ghio and P. Nagy, J. Mol. Struct., 187 (1989) 219.
[35] W. Zinth, M.C. Nuss and W. Kaiser, Phys. Rev. A, 30 (1984) 1139.
[36] M.I. Cabaço, M. Besnard and J. Yarwood, Mol. Phys., 750 (1992) 139.
[37] M.I. Cabaço, M. Besnard and J. Yarwood, Mol. Phys., 75 (1992) 157.
[38] K.N. Wong and S.D. Colson, J. Mol. Spectrosc., 104 (1984) 129.
[39] J.W. Emsley, J. Chem. Soc. (A), (1968) 1387.
[40] K.B. Wiberg, V.A. Walters, K.N. Wong and S.D. Colson, J. Phys. Chem., 88 (1984) 6067.